 https://doi.org/10.18171/1.094114

Capabilities of satellite radar measurements to map large-scale flooding [Satellite flood mapping]

Henriette Sudhaus

Karlsruhe Institute of Technology, Geophysical Institute, henriette.sudhaus@kit.edu

Summary

In October 2023 the German coasts of the Baltic Sea experienced a rare storm flood event. Significant infrastructure damages have been caused directly at the coast and further inland. Furthermore, some of the coastal protection infrastructure did not withstand the water pressure and/or duration of the flood everywhere and failed in parts. As a consequence, some protected low-elevation areas got flooded. There the retreat of water is hampered and they remained flooded even after the Baltic Sea water levels returned to normal. In terms of risk these areas require a different attention than places directly at the coastline, because flooding may be less frequent but of longer duration.

While locally the extent of the flooding has been witnessed and recorded in detail, assembling the big picture in a timely fashion across the landscape is difficult. Space-borne remote sensing can be of service here. In this study I demonstrate the potential of detecting and mapping the flooding of land surface with space-borne synthetic aperture radar images and methods of change detection as well as image segmentation. While for the October 2023 flood, space-borne radar images have only been recorded 18 to 20 hours after the peak of the flood and when the open sea water level had already returned to normal, a large area evidently remained flooded and could be mapped. Among them are several large flooded areas along the shores of the Schlei estuary up-river to the town of Schleswig and much further east between the mainland and the Darß peninsula. Notable is as well that even 12 days later, on November 2, a not negligible part remained flooded.

In this study, I augment the detections of flooding with complementary and open spatial data that provide information on elevation and infrastructure. The methods presented are not new, but show a general applicability and large potential if exploited. With rising sea levels, storm floods will likely occur more often with such severity. At the same time we may expect the means of satellite observations to improve in the future.

Keywords

Storm flood, space-borne Synthetic Aperture Radar, SAR, change detection

Zusammenfassung

Im Oktober 2023 fand eine seltene Sturmflut an der deutschen Ostseeküste statt. Dabei wurden nicht nur direkt an der Küste, sondern auch recht weit im Landesinneren signifikante Schäden verursacht. Einige Schutzdeiche hielten dem Wasserdruck und/oder Dauer des hohen Wasserstandes nicht stand und brachen, weshalb auch tiefliegende Bereiche hinter den Deichen geflutet wurden. In diesen Bereichen hielt die

Received 18. December 2024, reviewed 3. January 2025, revised 28. May 2025, accepted 28. May 2025, available online 11. August 2025.

Überflutung zudem länger an als die Sturmflut selbst, weil der Rückzug des Wassers hier erschwert war. In Bezug auf das Risiko benötigen diese Bereiche daher eine andere Berücksichtigung als die exponierten Gebiete direkt an der Küste.

Die Ausmaße dieser Sturmflut wurden mancherorts direkt beobachtet und detailliert aufgenommen. Eine rasche großräumige Zusammenstellung aller überfluteten Bereiche und der gesamten Überflutungsfläche ist jedoch schwierig. Satellitengestützte Fernerkundung kann hier gute Dienste leisten. In dieser Fallstudie demonstriere ich welches Potential die Detektion und das Kartieren von Überflutungen mit Aufnahmen von synthetischem Apertur Radar (SAR) in Kombination mit Methoden der Veränderungsdetektion und Bildsegmentierung haben. Für die Ostseesturmflut im Oktober 2023 wurden satellitengestützte SAR Aufnahmen erst 18 bis 20 Stunden nach dem Höchststand der Flut gemacht, zu einer Zeit, als der Wasserstand der Ostsee schon auf sein normales Level zurückgefallen war. Trotzdem konnten große Flächen identifiziert werden, die weiterhin überflutet waren. Darunter sind einige Gebiete entlang der Schlei bis hin zur Stadt Schleswig, aber auch weit östlich davon, zwischen der Halbinsel Darß und dem Festland. Bemerkenswert ist weiterhin, dass auch bis 12 Tage danach, am 2. November 2023 und später, viele Bereiche noch überflutet blieben.

In meiner Fallstudie kombiniere ich die Detektionen von Überflutungen mit ergänzenden und frei zugänglichen Raumdaten, zum Beispiel mit hochaufgelösten Höhenmodellen und Infrastrukturdaten. Die hier präsentierten Methoden sind nicht neu, jedoch gekennzeichnet durch eine allgemeine Anwendbarkeit und ein großes Entwicklungspotential. Letzteres ist auch dadurch gegeben, dass wir mit zunehmenden Möglichkeiten der Satellitenbeobachtung in der Zukunft rechnen können.

Schlagwörter

Sturmflut, satellitengestütztes Synthetische Apertur Radar (SAR), Veränderungsdetektion

1 Introduction

The storm flood of October 2023 arrived on top of an already days-lasting high water level in the Baltic Sea of a few tens of centimeters above average according to a report by the Bundesamt für Seeschifffahrt und Hydrographie (BSH 2023) on the storm flood on October 20, 2023 (Figure 1). At the German Baltic Sea coast this elevated water level ranged between 20 cm and 50 cm. The storm flood started on October 19 with wind directions turning to north-east and east in the central Baltic Sea according to the BSH (2023), which caused the water level to increase by another 130 cm in Kiel till 19:00 UTC (9 pm local time) on October 20. About three hours later another 10 cm higher water levels had been measured in Flensburg. At the coast of Mecklenburg-Western Pomerania the sea level increase reached not much higher than 150 m (Kiesel et al. 2024). Between 20:00 UTC and 23:00 UTC water levels dropped fast all along the German Baltic Sea coast, by about 200 cm within 21 hours at the western coast in Schleswig Holstein and 120 cm at the coast in Mecklenburg-Western Pomerania.

During the October 2023 flood, infrastructures that are naturally exposed to the coast and sea water like harbours have been heavily affected (NDRa 2023). Furthermore also some low-elevation and in principle protected areas were flooded because dykes failed, for instance near Arnis in Schleswig-Holstein (NDRb 2023) and near Wieck a. Darß in Mecklenburg-Western Pomerania (Nordkurier 2023). Special areas are the Geltinger Birk, a historical site of claimed and with dykes protected land, and the wide, lake-like estuary of the

river Schlei in Schleswig-Holstein (Figure 1), which has a narrow entry to the sea near Maasholm. Here, any water in- and outflow may be slowed down. During the October 2023 storm flood the water levels increased similarly fast in Schleswig at the river Schlei compared to measurements at the open water coast, but decreased much slower (NDRc 2023, Figure 1b). In Schleswig, the high water level peaked later at 2.33 m, remained longer and a normal water level was only restored almost a day later than elsewhere (Figure 1b).

For several other low-elevation areas protection dykes had been insufficient and/or failed (NDRa 2023, NDRc 2023, Nordkurier 2023). Also in these cases a high water level remained long after the sea level had dropped back to normal, because either the land surface behind the protection dykes is very low compared to sea level and/or because the outflow is hampered and slow. Mapping these areas efficiently on a large scale helps to assess damages and to organize immediate and long-term mitigation measures.

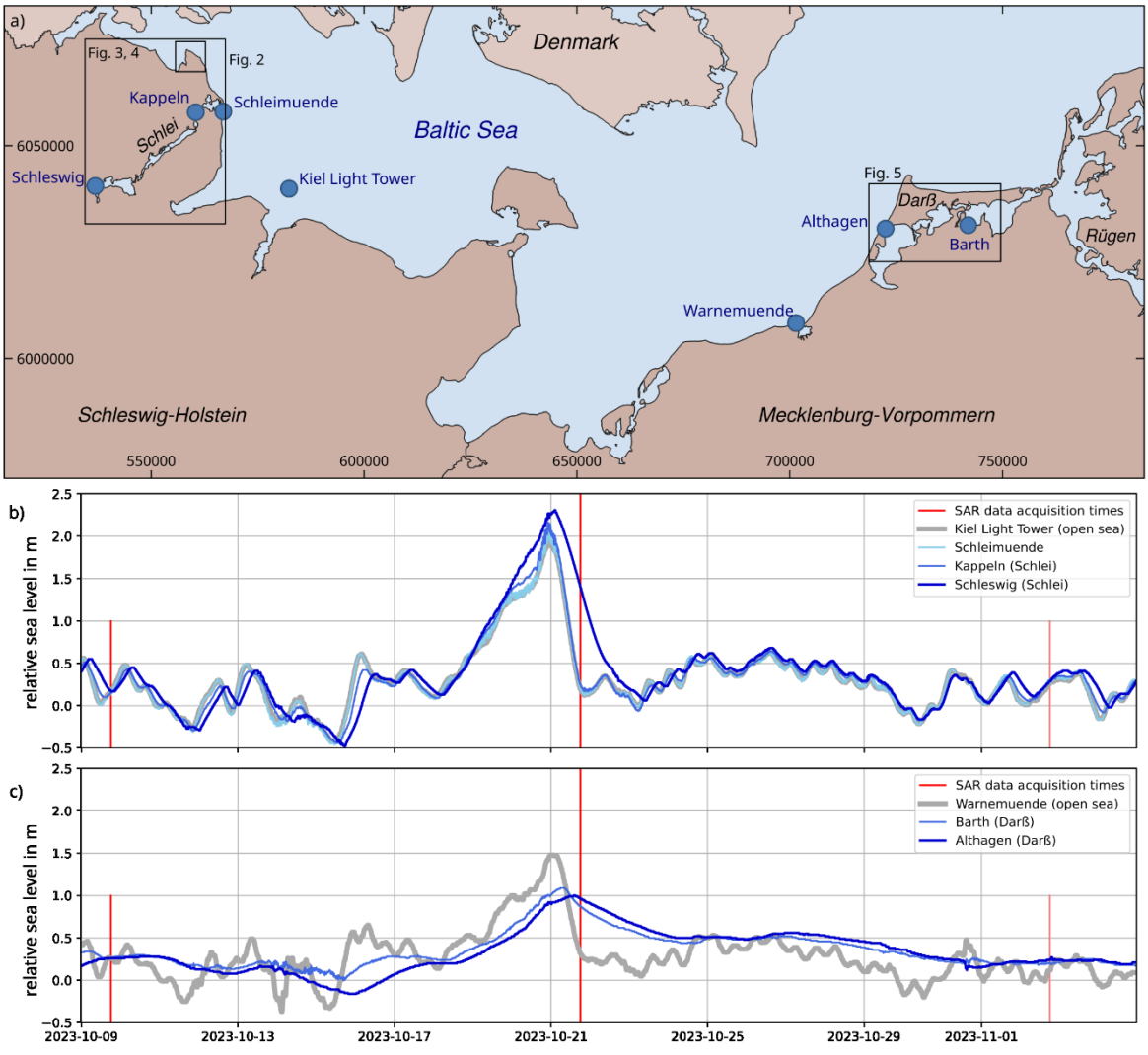

Figure 1: a) Map of the German flood affected coastal areas, b and c) 26 days of water level data before and after the flood (reported by the Wasserstraßen- und Schifffahrtsverwaltung Germany, WSV) for the coast in (b) Schleswig-Holstein and (c) in Mecklenburg-Western Pomerania. Red vertical lines mark the acquisition dates and times of the used satellite data. Map coordinates are in UTM, zone 32.

Mapping flood affected areas based on remote sensing data has been done since data have been available from satellites (e.g. Choudhury 1989), with an ever increasing spatial resolution. In this study I use data from the Sentinel-1 radar satellite operated by the European Space Agency (ESA) and apply change detection methods to map flooding. Radar waves are not absorbed by the atmosphere nor by cloud cover, which is very relevant for imaging the Earth's surface during all-weather conditions, in particular storms. Sentinel-1 satellites emit pulsed radar waves in C-band (radar wavelength λ=5.6 cm) and record wave energy that is backscattered from the Earth's surface.

A natural land surface is rough compared to the radar wavelength based on the Rayleigh criterion (Peake and Oliver 1971) and scatters considerable wave energy back to the satellite. Inland areas covered by water generally form smooth surfaces that mostly reflect radar energy away from the satellite and scatter much less back to the satellite. Therefore, over water surfaces, a generally lower backscatter amplitude is observed compared to land surfaces (Figure 2). This contrast in backscatter energy is spatially more stable in cross-polarized images (Tran et al. 2022). These images provide only recordings of backscattered waves that have a 90 degree polarization angle compared to the vertically polarized emitted signals. Only rough surfaces produce significant scattering with polarization changes. In vertically co-polarized images partially flooded areas may lead to an increased backscatter amplitude that makes the interpretation more complex (Manjusree et al, 2012; Tran et al. 2022). I exploit the cross-polarized amplitude difference in images acquired before, during and after the flood to map flooded areas (Figure 2).

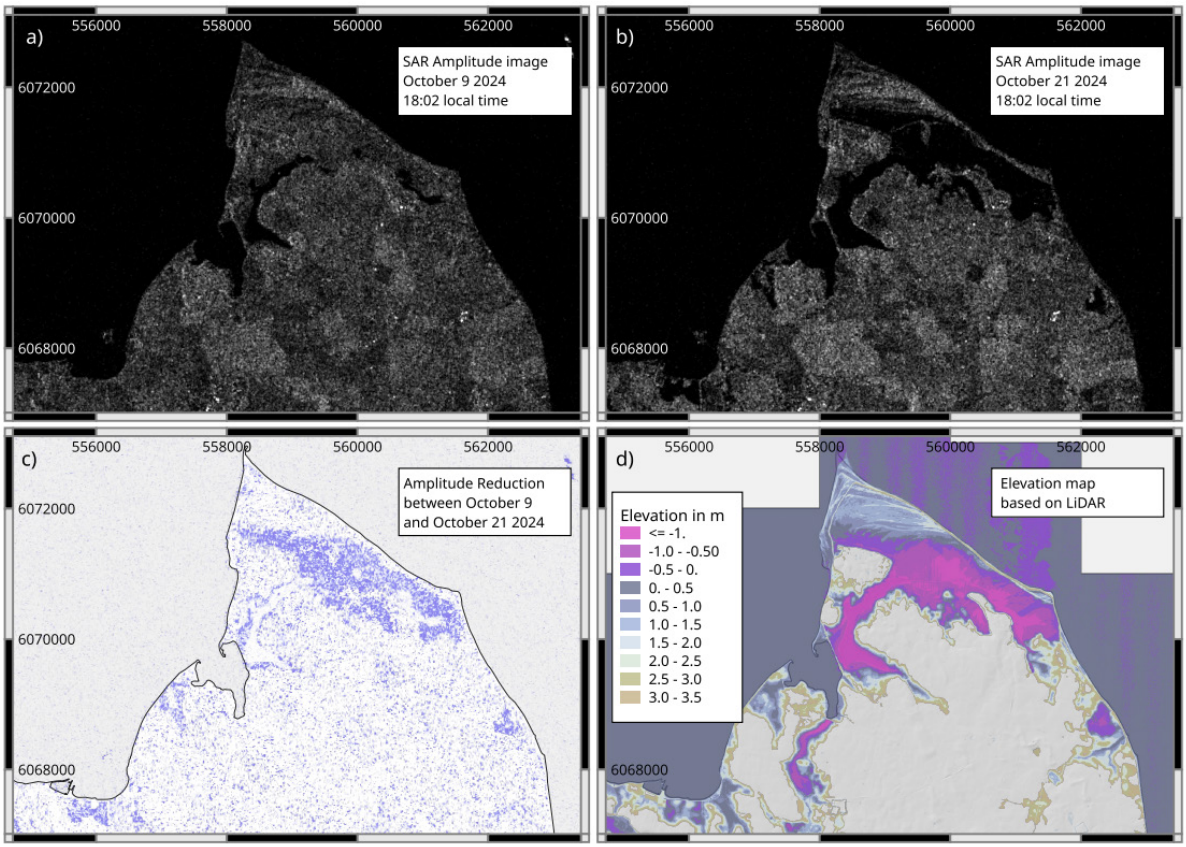

Figure 2: Principle of flood mapping shown for the Geltinger Birk (see Figure 1a). SAR amplitude images shown are acquired a) on October 9 and b) on October 21. c) Amplitude reduction of 30 % and more is shown in blue. d) High-resolution DGM1m elevation map of Schleswig-Holstein. Map coordinates are in UTM, zone 32.

Not always are flooded areas forming smooth water surfaces and not always are temporary water-covered surfaces caused by flooding, but also by rain. In this study I use Digital Elevation models for support in classifying detected change. Furthermore, at the time of the October 2023 storm flood the Sentinel-1 mission was short of one of two satellites, doubling the so-called revisit time between acquisitions of the same viewing geometry to only every 12 days. As an effect, only for a single satellite track suitable acquisitions during the flood event are available. This acquisition took place on Saturday (October 21) between 17:01 UTC and 17:02 UTC (7:01 pm local time), about 21 hours after the peak of the flood on Friday night (October 20) around 20:00 UTC (10 pm local time). At this time, the sea level near the coast had already dropped to a normal water level (Figure 1b and c). Along the Schlei and the water area enclosed by the Darß peninsula and the mainland the water level was still high during this image acquisition. Measured water levels above normal were 1.33 m in Schleswig at the Schlei river, 0.95 m in Althagen on Darß and 0.85 m in Barth (Figure 1). Therefore many areas with remaining flooding could be detected in the SAR images.

2 Data and Methods

I use the Sentinel-1 Level-1 georeferenced ("GRD") products with a spatial resolution of 8 m in east and 15 m in north direction, provided by ESA via ESA's Copernicus EO browser. As additional data I use the high-resolution digital elevation models and Openstreetmap & Contributors (OSM) data. The digital elevation models are based on airborne LiDAR (Light Detection and Ranging) and have a 1 m spatial resolution. They are provided by the federal states of Schleswig-Holstein and Mecklenburg-Vorpommern as open geodata.

To map reduction of backscatter energy caused by flooding I calculate the two differences in the SAR amplitude images for the acquisitions 10 days before the flood (October 9) with the image hours after flood peak time (October 21, 17:02 UTC) and with the image 12 days after the flood event (November 2) (Figure 2). I normalize these two amplitude differences by the amplitudes of the pre-flood image of October 9 2023. Positive differences mark amplitude reductions for the later acquisitions, with an unlikely maximum value of 1, which would mean the backscatter amplitude has been reduced to a perfect zero. Negative values (amplitude increase) are discarded as random or other effects. I also discard small positive values below 0.3, which correspond to an amplitude reduction of only 30 % that could likely be caused by random effects. I found that below this threshold many pixels would be counted in that are situated in open sea areas and show clear random intensity changes. Increasing the threshold reduces the density of flood detections in reportedly flooded areas. Figure 2c shows this intermediate result for the Geltinger Birk. Prominent is a high density of amplitude-reduced pixels in the low elevation areas of the Geltinger Birk (Figure 2d). There are spurious randomly distributed amplitude reductions, spanning one or few pixels over land and over water surfaces. I consider these as spatial noise in the amplitude due to random changes of the backscatter characteristics of the surface and instrument noise at the radar antenna. To reduce this noise I apply a Gaussian-weighted spatial average with the window length of 10 pixels using the Python numpy library (Harris et al. 2020). As a consequence, I loose resolution and may miss very small-scale flooding, but I achieve a much clearer imaging.

In a next step I remove amplitude reductions or flooding detections that occurred on land with an elevation higher than the maximum level observed by tide gauges, which were at a 2.33 m in Schleswig and 1 m for the Bodden area at Darß peninsula (Figure 1). Any detections from an elevation of 2.33 m and higher can be regarded as rain water-covered meadows and/or farmland or alternatively been altered by a farming procedure to a significantly smoother surface between the radar image acquisitions. I remove spurious detections over normally water-covered areas as well. For these steps I apply standard tools of the open-source QGIS project and skimage python toolbox (Van der Walt 2014).

To map the land areas still flooded 12 days after the flood peak, I repeat the same steps of image processing described before with the SAR images acquired on October 21 and November, with one difference. Areas that were flooded during the image acquisition on October 21 and which remain flodded till the next image acquisition on November 2 show a similarly low backscatter intensity in both images. Areas that dried in between the acquisitions show an intensity increase of backscatter. Therefore the detection runs on positive change values.

Since flooding of areas within settlements or otherwise developed areas with valuable infrastructure is of particular interest, I augment the flood detections with elevation data and open spatial data, in particular OSM data. Combining both these data sets, I can determine how much of a residential neighbourhood or otherwise build-up area or forest covered land is situated at low elevation and therefore possibly exposed to flooding, but not easily detected as such by using change detection in SAR images. Additionally, if flooding is detected near a build-up area that is situated below the previously determined water level, streets are likely flooded as well, while not detected as explained above. Therefore, I mark low-elevation areas simply by clipping the digital elevation data at the determined water level and the shoreline. Then I apply the image segmentation method of water-leveling to separate and mark low-elevation areas that are spatially connected. For both techniques I employ tools of the Python skimage toolbox. To determine which low-elevation areas are actually connected the high resolution of the elevation models is required. This is because these areas are often protected with a network or cascade of dykes, build to prevent large scale flooding. If flooding is detected within such a connected low-elevation, it very likely affects the entire depression. Possible blind spots of the detection method are discovered in this way. Here, I restrict the marking of connected low-ground areas to areas with significant coverage of at least 10000 m² (the area of about 90 connected pixels and more) for clarity in the illustration.

3 Detected flooded areas

The flood detections based on SAR images reveal all heavily affected areas covered in media reports. Furthermore, based on the flood detections and the elevation models, I can visually estimate the water level for the Schlei estuary at 17:02 o'clock UTC on October 21 to be still about 1.2 m higher than normal. Tide gauge data in Schleswig measured a water level of 1.33 m above normal for that time, while closer to the open sea, in Kappeln, the data show already a close to normal water level (Figure 1b). As a consequence, areas with a lower elevation and not protected by dykes remained flooded, also 20 hours after the flood peak (Figure 3a). There is extended flooding along the Schlei river. Mostly, the flooding affects meadows and farmland. Settlements most often are situated at high enough

elevation to not be affected by storm floods of the 2023 category. Still, significant flooding is detected near the towns Arnis and Schleswig (Figure 3b, c), which reaches very close to buildings. On November 2 2023, 13 days after the peak of the flood, some areas are still flooded, including the protected low-elevation area on the Geltinger Birk as well as close to Arnis (Figure 4a).

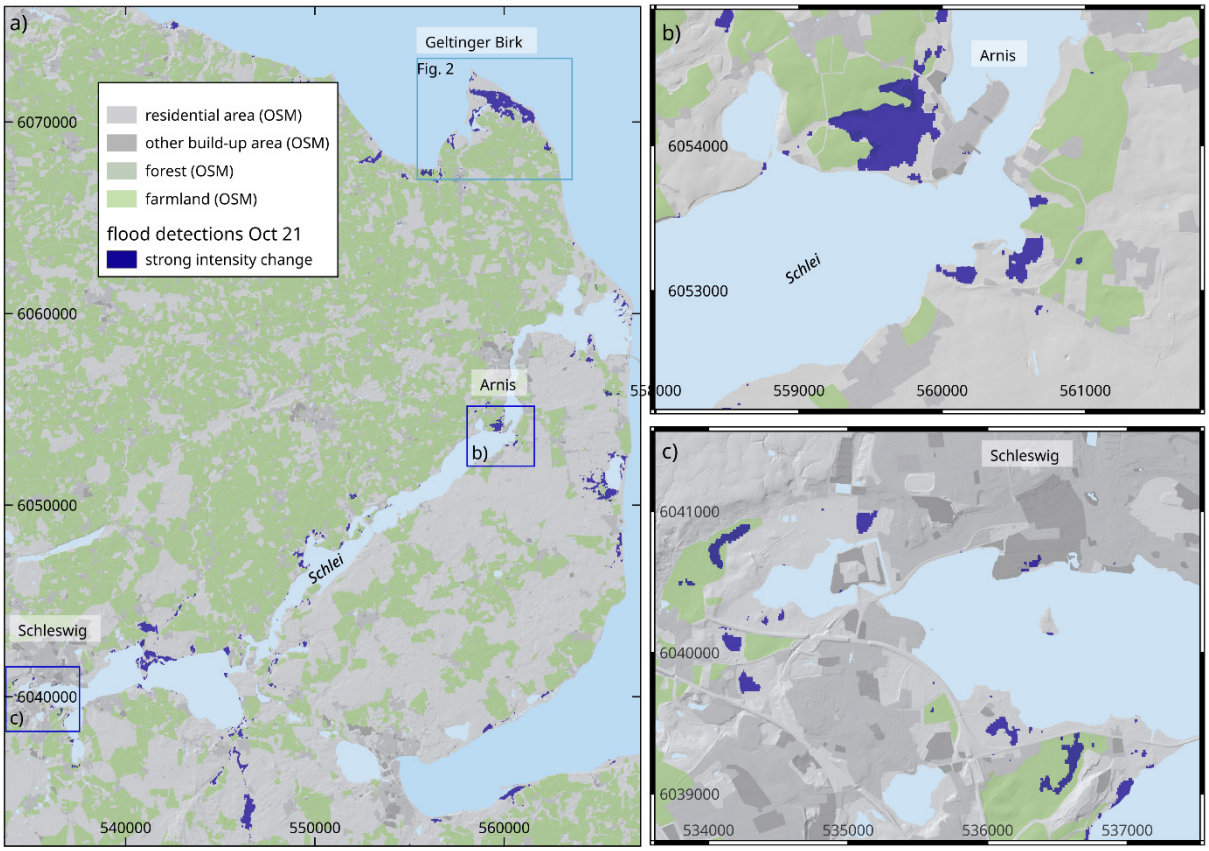

Figure 3: a) Flood detections at the river Schlei on October 21 in 2023 at 17:01 UTC, with a focus on the towns of b) Arnis and c) Schleswig where detected flooding is threateningly close to buildings. a) The light blue box marks the location of the Geltinger Birk shown in Figure 2 and the dark blue boxes mark the regional location of b) Arnis and c) Schleswig. Map coordinates are in UTM, zone 32.

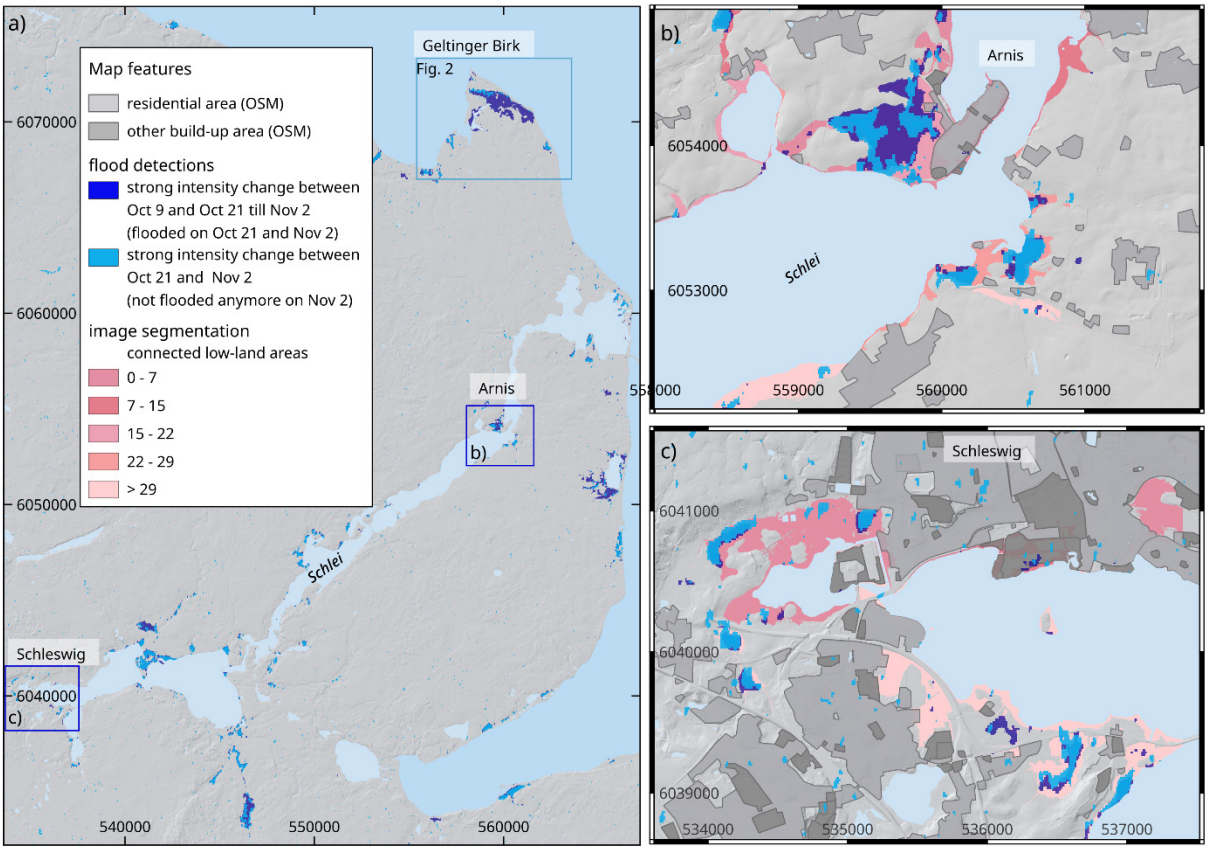

Figure 4: a) Flood detections including November 2 2023 17:01 UTC at the river Schlei, light blue colors depict flooded areas where water withdrew till November 2. b) and c) show close-ups and the results of image segmentation in light red colors near b) Arnis and c) Schleswig. Different light red colors mark individual connected low-elevation areas. Map coordinates are in UTM, zone 32.

At the Darß peninsula the water level between the peninsula and the mainland, the rather confined Bodden area, still reached a 0.9 m level above normal at the observation time 17:01 UTC, which is shown in tide gauge data (Figure 1c). Also here severe flooding is detected (Figure 5a). High water level threatened the village Wieck a. Darß (Figure 5b), where a dyke failed to protect the low land in one place because of a dyke breach and in another place due to overflowing (Nordkurier 2023). Furthermore, the wetland Große Kirr was entirely submerged at the observation time and in the western part of the Darß peninsula only a narrow dam remained above water connecting the peninsula to the mainland (Figure 5a). These flooding observations are consistent with the measured maximum water level and the water level at image acquisition time.

In Arnis, in Schleswig and in Wieck a. Darß residential buildings have been threatened by the storm flood. Based on the mapping made here, flooding of residential areas is very likely in Arnis and Schleswig. I demonstrate this by finding connected low-elevation areas. A large detected flooded area west of Arnis is situated in a larger vegetated depression below an elevation of 1.2 m, the estimated water level at observation time, into which some of the residential area is reaching (Figure 4b). Similarly, two patches of detected flooded area west of Schleswig are situated in the same, partly forested depression between the Tiergarten north of it and the Burgsee to the south (Figure 3c, Figure 4c). Likely, this depression was entirely flooded, but the radar backscatter remained high where the vegetation stands higher than the water level. A western, near-shore residential area of Schleswig is reaching into this depression, making a flooding of these parts of the town, based on this

method, very likely, too. Indeed, for Arnis and Schleswig flooding had been reported for the described areas during the peak time of the flood (NDRd 2023, NDRe 2023). Based on the detections here, it is likely that the water was still covering build-up ground at these two locations on the evening of October 21.

On Darß, near the western end of the village of Wieck a. Darß, a dyke failed to protect farmland from flooding due to one dyke breach and one part overflowing (Nordkurier 2023, NDR 2023). This flooding is well detected with the SAR change detection. The residential area does not reach below 0.9 m of estimated water level at the time of the observation and no damage in the village Wieck was reported. However, the detected area of flooding at this location is very likely strongly underestimated because the flooded farmland is bordered by an equally low-laying forested ground (Figure 5a, b). It is notable that the high resolution elevation model shows for the main dyke near Wieck tens of decimeter height undulations of the dyke crest, which appear to remain below 1 m in many parts and to get as low as 80 cm at the position of overflowing that is visible in media coverage (e.g. NDR 2023). The farmland flooding close to Wieck a. Darß withdrew till November 2 almost entirely. In contrast to that a similarly dyke-protected farmland area south of Wieck remains flooded till that day and likely longer.

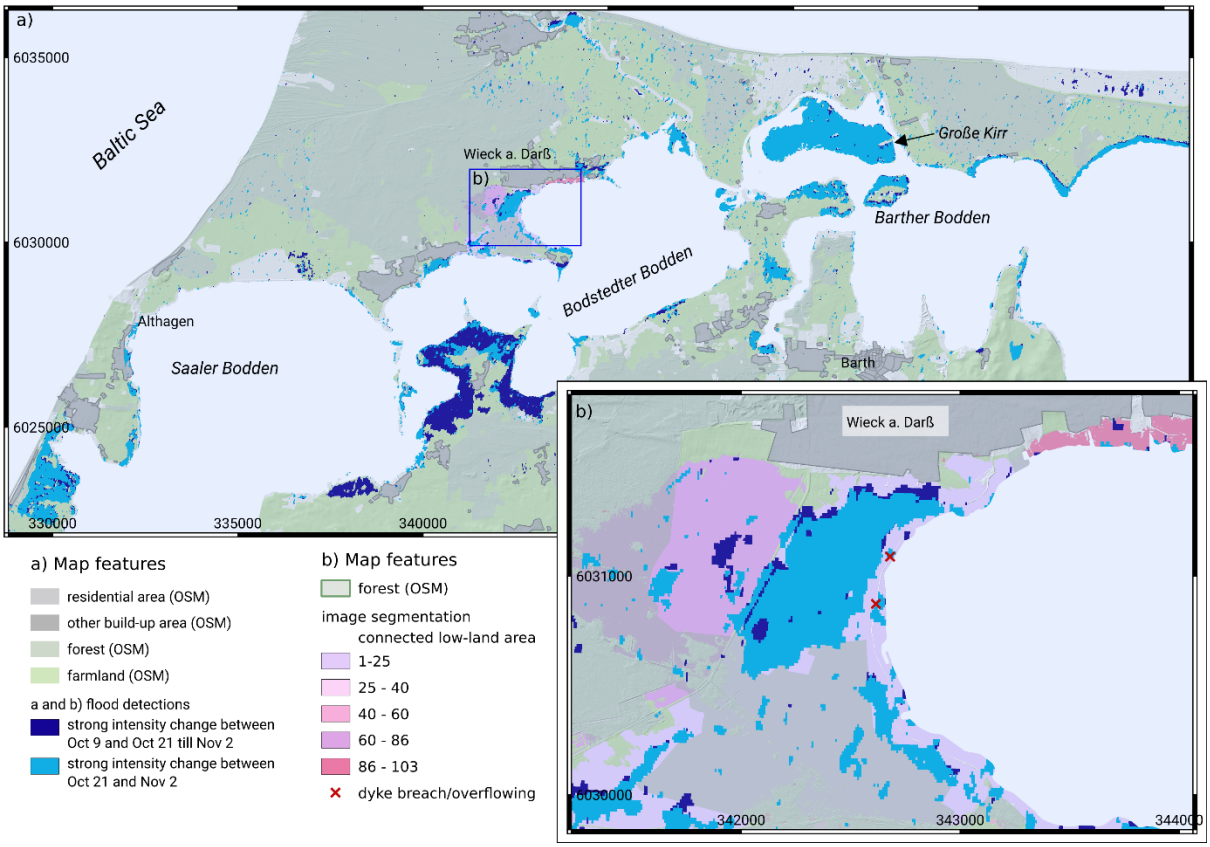

Figure 5: a) Flood detections on the Darß peninsula with a focus on b) the village of Wieck a. Darß. For location see blue box in a). b) shows the results of image segmentation in light red colors near Wieck. Different colors mark individual connected low-elevation areas. Map coordinates are in UTM, zone 33.

4 Discussion and Conclusion

Most critical for the here demonstrated assessment of damage through flooding are the restrictions in timing of the openly available SAR observations. The acquisition times are relatively sparse and can rarely be influenced in reaction to emergencies. The Sentinel-1 mission is a multi-purpose mission and mostly follows a strict space mission schedule for reliability. Further requirements that decrease flexibility in schedule stem from the satellite mission requirements of a sun-synchronous, low-earth orbit that realizes a global coverage. As a result, the acquisition times are mostly not optimal and revisit frequency is low for very dynamic processes as floods. It is only by chance therefore, that an acquisition takes place during or close to the peak time of a flood. For the October 2023 storm flood, a change detection based on SAR images became only possible 18 to 20 hours after the peak of the flood. This rather late observation was still timely compared to an effective revisit frequency of 3 days and therefore a rather lucky event. However, mapping lasting flooding is of importance, because damage is found to increase with long-term exposure to (salt) water for infrastructure and farmland (e.g. Kreibich & Dimitrova, 2010; Lazzarin et al., 2022). Additionally, these flood detections allow for the estimation of local water levels, where no direct measurements have been made.

The number of missions with space-borne SAR imaging has vastly increased in the last decade. One may hope for the trend towards an open-data policy by space agencies to continue. For instance the US Space Agency NASA plans launching an open-data SAR mission already in 2025, the NISAR mission, and ESA has just replaced the broken Sentinel-1B satellite in December 2024 by Sentinel-1C. Since 2025, the nominal revisit period of Sentinel-1 over Europe is therefore back to 6 days compared to the 12 days revisit in October 2023. Also very relevant in the context of emergency response are satellite data of the increasing number of missions with restricted data and commercial missions. For both, data are regularly made available, and acquisitions are even tasked in support of emergency response.

A further limitation of the presented flood detection method is that it fails for some surface coverage, e.g. for forests and build-up areas, as demonstrated. The presented very direct approach of change detection in radar image amplitudes may fail to show even significant flooding when not all objects on the ground become completely submerged. Then the required smooth surface is not realized (Amitrano et al. 2024). For example, in flooded forests trees will still be mostly above ground and the negative effect on the radar wave backscatter could be negligible. Similarly in settlements and build-up areas, where the associated risk of a flood is particularly high, the change in backscatter may be small. In these cases the described method has blind spots and false negatives in detection will occur (Amitrano et al. 2024). False positive detections can occur as well. In the days and weeks before the October 2023 Baltic Sea storm flood, high precipitation put several fields under water. False positives in flood detection can be discovered as such by taking into account complementary data, first of all elevation models. For instance, elevation models reveal whether a detection shows flooding for relatively high elevation, which points to rain-inflicted flooding. In a more detailed analysis than presented here, the additional processing of the co-polarized VV backscatter component of Sentinel-1 data could be used, which may allow to identify partially flooded land through an increase of backscatter due to effective double-bounce effect (Manjusree et al 2012, Tran et al. 2022).

Augmenting the change detections with complementary data helps to mitigate the amount of missing detections. Therefore, the presented flood detection method based on space-borne SAR imagery has a high potential to gain a large-scale spatial overview over flood-affected areas. The method is in principle easy and easy to implement, not least of all because the data sets used here are open data. Many analyses, like the image segmentation I presented, can be done beforehand and stored to be directly used in a fast and high-quality response to an emergency.

5 References

Amitrano, D.; Di Martino, G.; Di Simone, A.; Imperatore, P.: Flood detection with SAR: A review of techniques and datasets. In: Remote Sensing, 16, 4, 2024.

Bundesamt für Schifffahrt und Hydrographie: Report on the storm flood on October 20, 2023, by the Bundesamt für Seeschifffahrt und Hydrographie. https://www.bsh.de/DE/THEMEN/Wasserstand_und_Gezeiten/Sturmfluten/_Anlagen/Downloads/Ostsee_Sturmflut_20231020.pdf?__blob=publicationFile&v=2 accessed 2025-05-26.

Choudhury, B. J.: Monitoring global land surface using Nimbus-7 37 GHz data Theory and examples. In: International Journal of Remote Sensing, 10(10), 1579–1605, https://doi.org/10.1080/01431168908903993, 1989.

ESA Copernicus EO browser: https://browser.dataspace.copernicus.eu.

Flanders Marine Institute Report: Intergovernmental Oceanographic Commission (IOC): Sea level station monitoring facility, http://www.ioc-sealevelmonitoring.org accessed 2024-09-25, https://doi.org/10.14284/482, 2024.

Geodaten DGM1 of Mecklenburg-Vorpommern: https://laiv.geodaten-mv.de/afgvk/Geotopographie/Download?produkt=DGM1, accessed in 2024.

Geodaten DGM1 of Schleswig Holstein: https://geodaten.schleswig-holstein.de/gaialight-sh, accessed in 2023.

Harris, C. R.; Millman, K. J.; van der Walt, S.J. et al.: Array programming with NumPy. In: Nature 585, 357–362, https://doi.org/10.1038/s41586-020-2649-2, 2020.

Kreibich, H.; Dimitrova, B.: Assessment of damages caused by different flood types. In: WIT Transactions on Ecology and the Environment, 133, 3-11, https://doi.org/10.2495/FRIAR100011, 2010.

Lazzarin, T.; Viero, D. P.; Molinari, D.; Ballio, F.; Defina, A.: A new framework for flood damage assessment considering the within-event time evolution of hazard, exposure, and vulnerability. In: Journal of Hydrology, 615, 128687, 2022.

Manjusree, P.; Prasanna Kumar, L.; Bhatt, C. M.; Rao, G. S.; Bhanumurthy, V.: Optimization of threshold ranges for rapid flood inundation mapping by evaluating backscatter profiles of high incidence angle SAR images. In: International Journal of Disaster Risk Science, 3, 113-122, https://doi.org/10.1007/s13753-012-0011-5, 2012.

NDRa: Bilder von der Ostsee-Sturmflut: So sieht es am Sonnabend aus, https://www.ndr.de/nachrichten/schleswig-holstein/sturmflut1790_backId-sturmflut-helfer100.html#content accessed 2025-05-26.

NDRb: Nach Sturmflut an Ostseeküste: Große Schäden, Aufräumarbeiten laufen accessed at https://www.ndr.de/nachrichten/schleswig-holstein/Nach-Sturmflut-an-Ostseekueste-Grosse-Schaeden-Aufraeumarbeiten-starten,sturmflutostsee106.html, accessed 2025-05-26.

NDRc: Ostsee-Sturmflut: Geltinger Birk noch immer unter Wasser, accessed at https://www.ndr.de/nachrichten/schleswig-holstein/Ostsee-Sturmflut-Geltinger-Birk-noch-immer-unter-Wasser,geltingerbirk148.html, accessed 2025-05-26.

NDRd: Ostsee-Sturmflut: Aufräumen in Arnis, accessed at https://www.ndr.de/nachrichten/schleswig-holstein/arnis202_backId-arnis198.html#content, accessed 26-05-26.

NDRe: Bilder von der Ostsee-Sturmflut: So sah es in Schleswig-Holstein aus, accessed at https://www.ndr.de/nachrichten/schleswig-holstein/Ostsee-Sturmflut-So-sieht-es-in-Schleswig-Holstein-aus,sturmflut1588.html, accessed 2025-05-26.

Nordkurier: Deichbruch auf dem Darß – Wasser bedroht 75 Wohnhäuser, accessed at https://www.nordkurier.de/regional/mecklenburg-vorpommern/deichbruch-auf-dem-darss-wasser-bedroht-wohnhaeuser-1993420, accessed 2025-05-26.

Openstreetmap, © OpenStreetMap contributors.

Peake, W. H.; Oliver, T. L.: The response of terrestrial surfaces at microwave frequencies, Defense Technical Information Center, 1971.

QGIS Development Team (2024). QGIS Geographic Information System. Open Source Geospatial Foundation Project. http://qgis.osgeo.org.

Tran, K. H.; Menenti, M.; Jia, L.:Surface water mapping and flood monitoring in the Mekong Delta using sentinel-1 SAR time series and Otsu threshold, In: Remote Sensing, 14(22), 5721, https://doi.org/10.3390/rs14225721, 2022.

Van der Walt, S.; Schönberger, J. L.; Nunez-Iglesias, J.; Boulogne, F.; Warner, J. D.; Yager, N.; Yu, T.: scikit-image: image processing in Python. In: PeerJ, 2, e453, https://doi.org/10.7717/peerj.453, 2014.

WSA: short message on the storm flood on October 20, 2023: https://www.wsa-ostsee.wsv.de/Webs/WSA/Ostsee/DE/SharedDocs/Kurzmeldungen/2023_11_28_Sturmflut_Oktober_2023.html.